Microwave-Assisted Rapid Photocatalytic Degradation of Malachite Green in TiO_2 Suspensions: Mechanism and Pathways

Yongming Ju, Shaogui Yang,* Youchao Ding, Cheng Sun,* Aiqian Zhang, and Lianhong Wang

State Key Laboratory of Pollution Control and Resource Reuse, School of the Environment, Nanjing University, Nanjing 210093, P.R. China

Received: May 20, 2008; Revised Manuscript Received: July 14, 2008

Microwave-assisted photocatalytic (MPC) degradation of malachite green (MG) in aqueous TiO_2 suspensions was investigated. A 20 mg/L sample of MG was rapidly and completely decomposed in 3 min with the corresponding TOC removal efficiency of about 85%. To gain insight into the degradation mechanism, both GC-MS and LC-ESI-MS/MS techniques were employed to identify the major intermediates of MG degradation, including *N*-demethylation intermediates [(*p*-dimethylaminophenyl)(*p*-methylaminophenyl)phenylmethylium (DM-PM), (*p*-methylaminophenyl)(*p*-methylaminophenyl)phenylmethylium (MM-PM), (*p*-methylaminophenyl)(*p*-aminophenyl)phenylmethylium (M-PM)]; a decomposition compound of the conjugated structure (4-dimethylaminobenzophenone (DLBP)); products resulting from the adduct reaction of hydroxyl radical; products of benzene removal; and other open-ring intermediates such as phenol, terephthalic acid, adipic acid, benzoic acid, etc. The possible degradation mechanism of MG included five processes: the *N*-demethylation process, adduct products of the hydroxyl radical, the breakdown of chromophores such as destruction of the conjugated structure intermediate, removal of benzene, and an open-ring reaction. To the best of our knowledge, it is the first time the whole MG photodegradation processes have been reported.

1. Introduction

As a cationic triphenylmethane dye, malachite green (MG) not only has been extensively used in the textile industry for dyeing wool and silk,[1] but also has a widespread use in the paper, leather, and pharmaceutical industries. Consequently, MG with relatively high levels is always present in industrial wastewaters, and is harmful to human and others due to its genotoxic and carcinogenic properties,[2,3] through accumulating in fat tissue to form in bioaccumulation and further inducing even great toxicity than usual medical disinfectant residue as biocide as testified. Thus, it is of particular significance to efficiently remove MG from wastewaters before their discharge into the receiving waters. Unfortunately, the conventional biological treatment processes can not effectively remove dyes from textile waster, due to the resistance to biological degradation.[4,5] In addition, other chemical and physical treatments, such as flocculation, ultrafiltration, adsorption, ozonation, and chlorination,[6] are not efficient since they create other environmental problems and so on. Therefore, it is necessary to explore an effective method of wastewater treatment to remove hazardous dyes from waste streams.[5]

Some promising technologies assisted by microwave technique have been developed to treat efficiently the contamination,[7,8] since the application of microwave energy was reported in the field of environmental remediation.[9,10] One of the newly proposed effective methods is the microwave-assisted photocatalytic process (MPC), which contains a suitable photocatalyst[11−14] to utilize the UV irradiation of electrodeless discharge lamps (EDLs) to degrade contamination. It is well documented that the TiO_2-based MPC technology has been used to degrade effectively pesticides,[15,16] dyes,[17,18] phenol,[19] and pentachlorophenol[20] and has the potential to be utilized in the treatment of industrial wastewater. This main reason is that the microwave could significantly improve the photocatalytic efficiency of TiO_2 for removal and mineralization of organic pollutants, as Satoshi Horikoshi[21] thought that a photocatalysis reaction induced by EDLs and microwave irradiation was proven to be higher efficiency than common photocatalysis. Up to now, there has been no report on MPC degradation of MG yet.

Meanwhile, the mechanism of MG photodegradation was also discussed from different viewpoints. Most studies believed that *N*-demethylation is a necessary step.[22] On the basis of the four kinds of *N*-demethylation intermediates detected under photocatalysis reaction of the 15 W−UV-365 nm lamp and P25 as catalyst, Chen et al.[23] solely performed the *N*-demethylation process. Supplying six kinds of intermediates by GC/MS under the condition of sonolytic, photocatalytic, and sonophotocatalytic degradation, Poulios[3] et al. proposed the parallel and competing pathways upon destruction of the conjugated structure and the *N*-demethylation reaction, without demonstrating the *N*-demethylation reaction and cleavage of aromatic ring reaction because of the limitations of the technique and analytical method employed. With the photolysis reaction under natural sunlight irradiation, detected by LC-TOF-MS and GC-MS, Agüera[24] et al. drew the conclusion that MG undergoes three main reactions such as *N*-demethylation, cleavage of the conjugated structure, and hydroxylation without the mentioned open ring reaction. Upon supplying more degradation products by GC/MS, catalyzed by Fe (III)-loaded resin in the presence of H_2O_2 at neutral pH values, Zhao[25] et al. proposed that the MG photodegradation was preceded by the cleavage of the central carbon of MG and followed by the *N*-demethylation process and opening of phenyl rings to form small molecular species. Actually, both the *N*-demethylation products and opening products of the ring were not observed. In theory, all the above reactions are possible for MG photodegradation. On the basis of the above analysis, we suggest that the whole MG photodegradation might involve five

* Corresponding author. Phone: +86-25- 83593239. Fax: +86-25-83593239. E-mail: envidean@nju.edu.cn (C.S.); yangdlut@126.com (S.G.Y.).

10.1021/jp804439z CCC: $40.75 © 2008 American Chemical Society
Published on Web 10/09/2008

processes: cleavage of the central carbon reaction, *N*-demethylation process, adduct reaction of hydroxyl radical on MG, removal of benzene, and opening of phenyl ring. To the best of our knowledge, however, there is still no report on the whole MG photodegradation mechanism involving all the above-mentioned processes.

In this study, we first reported the whole photodegradation mechanisms of MG in TiO_2 suspensions, which included cleavage of the central carbon reaction, *N*-demethylation process, adduct reaction of hydroxyl radical on MG, removal of benzene, and opening of phenyl ring.

2. Experimental Section

2.1. Reagents and Materials. P25 titanium was used as the photocatalyst, purchased from Degussa (ca. 80% anatase, 20% rutile; particle size, ca. 20−30 nm; BET area, ca. 55 $m^2\ g^{-1}$). MG ($C_{23}H_{25}N_2Cl$) was purchased from Sigma Company. HPLC-grade acetate acid and acetonitrile were purchased from Tedian Company. Deionized water was obtained by purification operation with a Milli-Q water ion-exchange system (Millipore Co.) to have a resistivity of $1.8 \times 10^7\ \Omega$ cm.

2.2. Apparatus. The whole apparatus used in these experiments has been referred to in the literature.[8,10,11] The apparatus, light intensity, and emission spectra of one electrodeless discharge lamp (EDL-1) are available in the Supporting Information (Figures 1S−3S). The leakage of the microwave (MW) oven was kept below 0.5 mW/cm^2 at 2450 MHz, which was measured at a 20 cm distance from the aperture, and was within the limit of the safe stray leakage of MW power density. Light spectra in the flask were measured using a Shimadzu UV-2100 spectrophotometer without any solvent. The main emission spectra of EDLs (in the wavelength range 200−800 nm) in the Supporting Information (Figure 3S) included 254, 296, 313, 364, 404, 435, 546, 576 nm; this is obviously different from that of EDLs reported in the literature,[26,27] with emissions at 365, 404, 435, 547, and 579 nm.

2.3. Experimental Procedures and Analysis Methods. Unless special explanations are noted, all experiments were carried out under the condition that the initial concentration of MG is 20 ppm with EDL-1, $C_{TiO2} = 0.1$ g/L, at an initial pH value of 4.2. Prior to irradiation of MG, all the dispersions were magnetically stirred in the dark for 30 min to establish the adsorption/desorption equilibrium between the solution and the catalyst surface and ensure the dissolved oxygen (DO) of solution has been saturated. A 50 mL portion of solution was put into the reactor vessel for several minutes of irradiation of EDLs, and then samples were drawn and immediately centrifuged (Beckman) at 20 °C, 10000 rpm, to remove catalyst particles from reaction solution for requirements of HPLC-ESI-MS/MS, HPLC, UV−Vis spectra, and total organic carbon (TOC) analyses.

During the experiments, LC-ESI-MS/MS was used to detect and identify polar degradation products such as MG and *N*-demethylated intermediates. GC-MS was used to detect nonpolar parts such as small molecules produced during the open ring reaction, and IC was used to detect the inorganic ions. HPLC (Agilent, 1100 series high-performance liquid chromatography) was equipped with a Zobax Extend-C18 HPLC column (150 mm × 6 mm using a C18 column i.d., 5 μm, Agilent), a diode array detector (DAD), and an auto sampler controlled by a Chemstation data acquisition system. Solvent A was aqueous ammonium acetate buffer (pH 4.5), and solvent D was ammonium. The measurement was performed in acetonitrile/water = 60:40 (v/v) as mobile phase with a flow rate of 1 mL/min and a detection wavelength of 618 nm. LC-MS (Thermo LCQ Advantages QuestLCQ Duo) was equipped with a Beta Basic-C18 HPLC column (150 mm × 2.1 mm i.d, 5 μm, Thermo). The mobile phase was acetonitrile/water (60:40, v/v). A 10 μL volume was injected using the autosampler. GC-MS (Finnigan Thermo) interfaced with a Polaris Q ion trap mass spectrometer was equipped with DB-5 fused-silica capillary column (30 m × 0.25 mm i.d, 0.25 μm film thickness). The oven temperature was programmed as follows: the initial temperature was 60 °C, then 60−300 °C at a ramp rate of 10 °C/min, held for 10 min. In MS analysis, the injector temperature and transfer line temperature were set at 250 and 200 °C, respectively. The ionization for MS was operated at 70 eV of electron impact (EI) mode with positive ion mode. The pretreated process was as follows: 20 mL of sample solution was extracted with 10 mL of n-hexane for three times, and the extracted solution was dehydrated using anhydrous sodium sulfate. Afterward, the dehydrated solution was concentrated to 1 mL. Before GC-MS analysis, trimethylsilylation was carried out at 50 °C for 30 min using 0.5 mL of bis(trimethylsilyl)trifluoroacetamide (BSTFA). IC (Dionex model ICS 1000 ion chromatography) was equipped with a dual-piston (in series) pump, a Dionex IonPac AS11-HC analytical column (4 mm × 250 mm), and a Dionex DS6 conductivity detector. Suppression of the eluent was achieved with a Dionex anion ASRS 300 electrolytic suppressor (4 mm) in the autosuppression external water mode.

3. Results and Discussion

3.1. Control Experiments of Microwave-Assisted Photocatalytic Degradation of MG. First, to demonstrate the role of MW and MW + TiO_2 within MPC, the results of control experiments were displayed in the Supporting Information (Figure 5S). Under only MW condition, there was no obvious change of concentration since the energy of the microwave (E = 0.4−40 kJ/mol at υ = 1−100 GHz) was not enough to destroy the bond of MG.[28] Under MW + TiO_2 condition, a similar result was observed. Obviously, the adsorption of MG was not able to decline the concentration of MG. Second, under the conditions of EDL + MW and EDL + MW + TiO_2, it could be found that the discoloration rate of the former was about 25.4% at 5 min with TOC removal of 9.5%, while that of the latter was 99% with the responding TOC removal of 85.1%, which demonstrated clearly the characters of MPC and the role of TiO_2. Combined with all of the above details, the higher removal efficiency of MPC was deduced due to the synergy effect of MW, EDLs, and TiO_2. During MPC operation, the microwave field could inhibit the recombination of photogenerated hole−electron pairs on the semiconductor surface and increase the transition probability of photon-generated electrons on the highly defected surface of the catalyst. Satoshi Horikoshi et al. proved,by electron spin resonance (ESR), that about 20% more ·OH was generated by photocatalysis with microwave irradiation than by photocatalysis alone.

3.2. UV−Vis Spectra. The variation of absorption spectra of MG during the MPC process was shown in Figure 1A, and the absorption spectra, partly enlarged (400−700 nm), were also illustrated in Figure 1B. The inset in Figure 1B described the structure of MG. It was apparently seen that the absorbance at 620 nm declined rapidly until it nearly disappeared at 3 min with a blue-shift of the maximum absorbance peak from 620 nm to about 598 nm. In addition, it was noted that the new absorbance peak appeared at about 360 nm. The absorbance peaks at 425 and 315 nm had obviously declined, which indicated the whole conjugated chromophore structure of MG

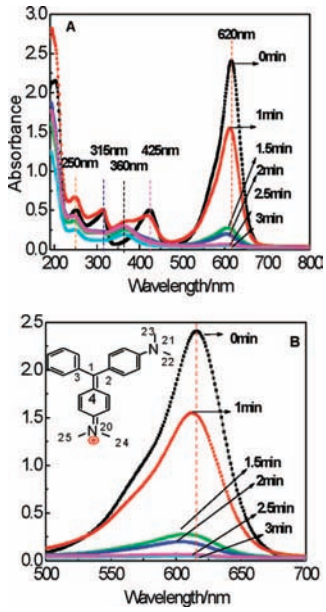

Figure 1. UV−vis spectra of MG after degradation (A) and the absorption spectra enlarged (B).

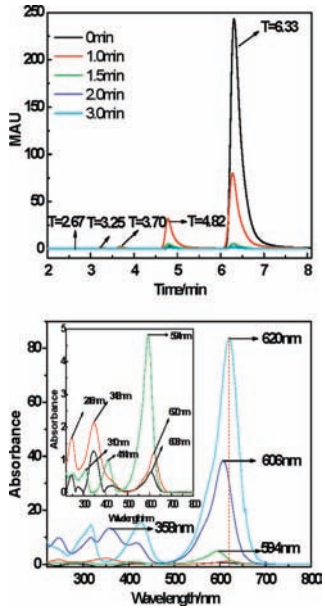

Figure 2. Chromatography of HPLC within 3 min with UV−vis spectra of responding peaks.

had been destroyed. From the above analysis, there might be competitive reactions between the cleavage of the central carbon reaction and *N*-demethylation reaction or other unfamiliar reactions at different reaction times, which compose the main part of the degradation mechanism.

3.3. Chromatography of HPLC within the MPC Process and Variation of Some Intermediates. After the degradation solution was separated, there were several peaks in HPLC chromatography with retention times (t_R) at 6.33, 4.82, 3.70, 3.25, and 2.67 min in Figure 2, accompanied with the UV−Vis spectra of the peaks mentioned above. The relative distribution of the intermediates after the MPC process is depicted in the Supporting Information (Figure 6S). Due to further oxidations, the intermediates underwent an increase first and then a decrease. Due to a lack of the standard materials of the above intermediates and the appropriate molar extinction coefficients, it was difficult to determine quantitatively all intermediates, so the distributions of all of the *N*-demethylated intermediates are intensities relative to the initial concentration of MG. The concentrations of intermediates underwent an increase first and then a decrease for further oxidations. However, there was not a stepwise photochemical process for the *N*-demethylation reactions.[19]

In Figure 2, products of degradation reactions were apparently displayed with the absorption spectra of each peaks varying from 620 to 594 nm; this supplied the most important convincing proof, according to the difference in UV−Vis spectra of MG and other degradation intermediates. Furthermore, the peaks with absorbance at 358 and 606 nm were consistent with the UV−Vis spectra after the reaction was carried out between 1.5 and 3.0 min in Figure 1, clearly different from others. The absorbance at 606 nm implied that the basic structure similar to MG existed, and the difference at 358 nm might originate from the adduct reaction of hydroxyl radical on MG. What is more, this reaction might be one of the main reaction routes. Similar results were observed at $t_R = 3.25$ min and $t_R = 2.67$ min, which might be produced through adduct reaction of hydroxyl radical on MG or *N*-demethylation reactions of adduct reaction of hydroxyl radical on MG. In terms of intensity relative to the initial MG concentration for comparison, the intermediate at $t_R = 4.82$ min might be produced through a major reaction than other *N*-demethylation reactions.

In the inset, the UV−Vis spectra responds with the peaks with t_R at 3.70, 3.25, and 2.67 min. The peak with $t_R = 3.70$ has absorbance peaks at 594, 414, and 310 nm, which could be deduced to the product of *N*-demethylation reactions. The peak with $t_R = 3.25$ has absorbance peaks at 620, 348, and 248 nm, which might be the adduct product of a hydroxyl radical, which could be oxidized into another product with absorbance of 608, 348, 248 nm with $t_R = 2.67$ min, both of which were first observed.

Thus, we could find that the blue shift was further verified by HPLC spectra of intermediates with the apparent blue shift from 620 to 606 nm, which confirmed that the blue shift originated from not only *N*-demethylation reactions, but also the reaction of an adduct of hydroxyl radical. The new peak in Figure 2 might result from the reaction of an adduct of hydroxyl radical to be identified.

3.4. Identification of the Intermediates of *N*-Demethylation Reaction and Adduct Products of Hydroxyl Radical. In the MPC process, numerous intermediates could be produced. According to the differences in polarity, the products via different reaction routes were detected by LC-ESI-MS/MS and GC-MS techniques separately. The UV−Vis spectra and HPLC analysis (shown in Figures 1 and 2) revealed that *N*-demethylation products were detected together with the parent compound after irradiation of several minutes. All the chromatographic peaks basically disappeared within 3 min.

N-Demethylation products are detected by an LC-ESI-MS/MS technique (Table 1). According to the results of mass spectral analysis, we assigned the following: A, $m/z = 329.4$ as MG with maximum absorption at 620 nm; B, $m/z = 315.4$ as (*p*-dimethylaminophenyl)(*p*-methylaminophenyl)phenylmethylium (DM-PM) with maximum absorption at 608 nm; D, $m/z = 301.3$ as (*p*-methylaminophenyl)(*p*-methylaminophenyl)phenylmethylium (MM-PM) with maximum absorption at 598 nm; E, $m/z = 287.5$ as (*p*-methylaminophenyl)(*p*-aminophenyl)phenylmethylium (M-PM) with maximum absorption at 589 nm. And F might be E's isomer. The results are consistent with others' reports; e.g., Agüera[21] et al. and Chen[18] et al. both identified the *N*-demethylated intermediates of B, D, and E by

TABLE 1: LC-MS Retention Time (t_R) and Spectral Characteristics of Products During the MPC Process

intermediate	m/z	t_R (min)	spectrum ions (m/z) (%, abundance)
A	329	4.38	329.4(100); 315(20); 251(40); 237(30); 208.2(55)
B	315	3.52	315.4(65); 301(15); 237.2(100); 223.3(75); 208.2(65); 194.2(45)
C	345	2.74	345.2(100); 274.2(20)
D	301	1.52	301.3(90); 287.1(10); 273.2(15); 223.3(100); 209.2(15); 194.2(70)
E	287	2.52	287.3(100); 273.4(12); 232(12); 218.5(15); 210.2(18); 209.2(36); 195.4(26)
F	287	2.81	287.5(56); 272.3(34); 256.3(10); 242.9(14); 229(26); 209.3(100); 194.3(16); 132.9(12)
G	273	2.51	273.2(100); 258.3(40); 240(65); 196(70)
H	361	2.26	345.3(50); 319.4(100); 315.6(15); 255.6(98); 240.4(80)
I	345	1.52	345.2(100); 262.9(15); 224.1(10)
J	327	1.61	327.3(100); 313.3(10)

an LC-MS technique under different conditions. In order to further identify these compounds, part of the above intermediates were first separated by HPLC and then identified by a HPLC-ESI-MS/MS technique in SIM mode.

A represents MG, and its major ions (m/z, %) in the mass spectra include the following: 329.2 (M; 100); 315.2 (M − CH_2; 10); 251.2 (M − C_6H_6; 38); 237.3 (M − C_6H_6−CH_2; 17); 208.2 (M − C_6H_6-2CH_2−NH; 56). B represents DM-PM, whose major ions (m/z, %) in the mass spectra include the following: 315.2 (M; 63); 301.2 (M − CH_2; 12); 237.2 (M − C_6H_6; 100); 223.2 (M − C_7H_8; 23); 208.2 (M − C_7H_9N; 66); 194.2 (M − $C_8H_{11}N$; 43). D represents MM-PM, its major ions (m/z, %) in the mass spectra include the following: 287.1 (M − CH_2; 5); 273.2 (M − C_2H_4; 5); 223.3 (M − C_6H_6; 100); 209.2 (M − C_7H_8; 11); 194.2 (M − $C_7H_{10}N$; 69). E represents M-PM, whose major ions (m/z, %) in the mass spectra include the following: 273.1 (M − CH_2; 45); 258.2 (M − CH_3N; 16); 209.2 (M − C_6H_6; 100); 194.2 (M − C_6H_7N; 22); 180.1 (M − C_7H_9N; 56). The demonstrated *N*-demethylated intermediates including A, B, D, E, and F were consistent with the literature.[18] However, there might be other reaction routes and reaction mechanisms which will be dicussed next. H represents the adduct products of two hydroxyl radicals. The major ions (m/z, %) in the mass spectra include the following: 345.3(50); 319.4(100); 315.6(15); 255.6(98); 240.4 (80). I represents adduct products of one hydroxyl radical. The major ions (m/z, %) in the mass spectra include the following: 345.2 (M; 100); 262.9(15); 224.1(10), both of which were first detected during photocatalytical degradations. However, their detailed information will be provided in a further study.

Besides these, other products were detected only by LC-ESI-SIM, and assigned $m/z = 313$ as K with the t_R of 3.60 min and $m/z = 299$ as L with the t_R of 4.43 min, which might be the byproducts of adduct products of one hydroxyl radical after *N*-demethylation reaction or dehydration reaction.

3.5. Identification of the Intermediates of the Cleavage of the Central Carbon and the Open Ring Reaction. Part of the intermediates were detected by GC-MS (Figure 3). All the products (in Table 2) were mainly produced through two reaction routes: the open ring reactions and the cleavage of the central carbon with the bond between C_1−C_4. The attack of hydroxyl radical resulted in the cleavage of MG and its

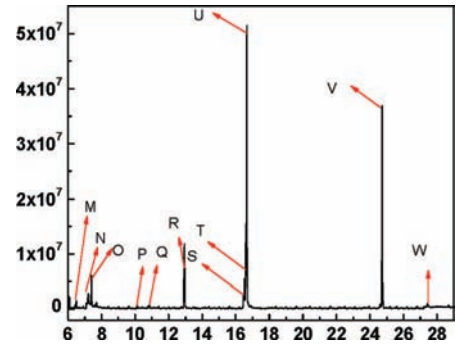

Figure 3. GC-MS chromatogram obtained from an extract of MG solution after 3 min of irradiation.

TABLE 2: GC-MS Retention Time (t_R) and Spectral Characteristics of Products During the MPC Process

Proposed intermediates		T_R (min)	EI-MS spectrum ions(m/z) (%, abundance)
M	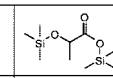	6.49	147(70); 117(70); 73(100)
N	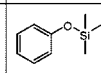	7.07	151(100); 166(30)
O		7.20	146(100); 111(40); 75(20)
P	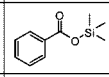	10.07	179(95); 135(55); 105(100); 77(80); 51(30)
Q	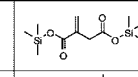	10.85	259(20); 147(100); 73(80); 45(20)
R	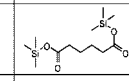	12.91	275(25); 147(40); 111(70); 73(100); 55(40); 45(25)
S	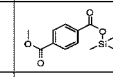	15.62	237(100); 221(20); 193(45); 163(40); 135(20); 103(20)
T	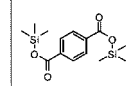	16.52	295(100); 251(20); 221(25); 135(20); 103(25); 73(20)
U	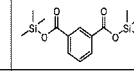	16.63	295(100); 251(20); 221(25); 135(20); 103(25); 73(20)
V	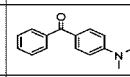	24.77	225(80); 148(100); 105(15); 77(20)
W	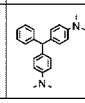	27.64	330(75); 286(15); 253(100); 237(10); 209(40); 165(25)

N-demethylation intermediates, and all the open ring products could be further oxidized into small organic molecules, even inorganic ions. Nevertheless, small molecular compounds such as HCOOH were not observed due to the evaporation during the sample preparation course.

Up to 11 kinds of chemicals were identified as the degradation intermediates of open ring reactions and the cleavage of the central carbon, after those peaks from the sample handling procedure and chromatographic system were discarded. Compounds labeled wit were occasionally detected, without being displayed in Table 2 but in Scheme 1. Due to the polarity difference, there were no peaks responding to MG and the *N*-demethylation intermediates. The molecular ion and spectrometric fragmentation peaks along with their relative abundance for different products were presented in Table 2. Products

SCHEME 1: Proposed Degradation Mechanism of MG During the MPC Process

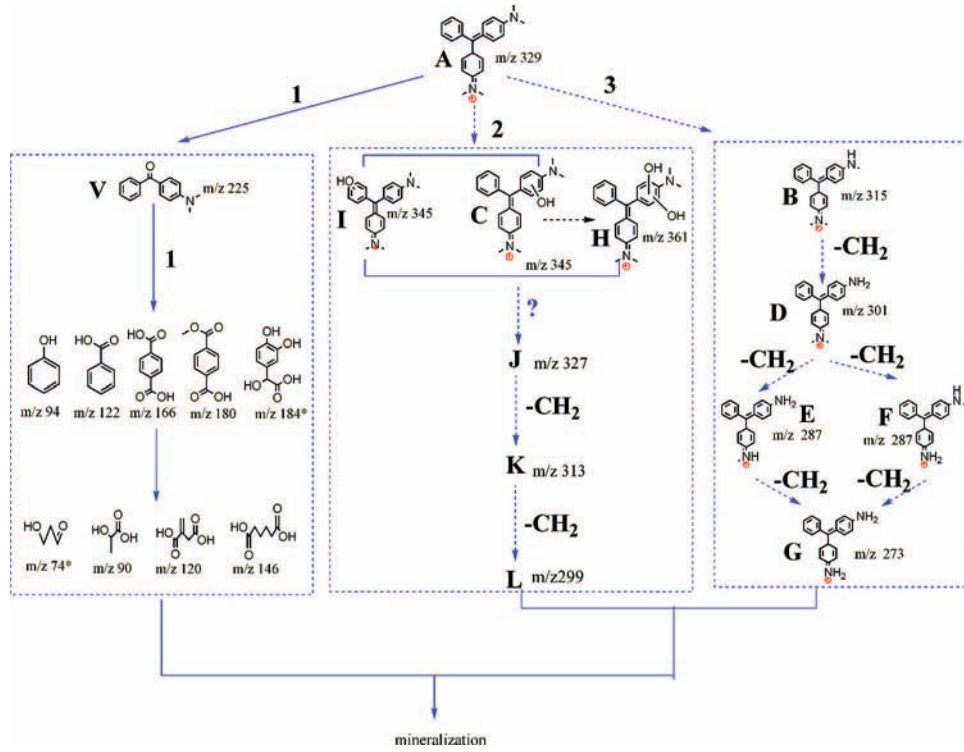

were identified by comparing the MS spectra with the responding products in NIST library.

As the intermediate of the central carbon cleavage, the peak with $t_R = 24.77$ min was detected by both LC-MS and GC-MS. The major ions in the mass spectra include the following (*m*/*z*, %): 225 (M, 80); 148 (M − C_6H_5, 100); 105 ($C_6H_5CO^+$); and 77 ($C_6H_5^+$, 20). A similar product was also found.[22] Then, the following reaction was the removal of the benzene reaction, which corresponded to the peaks with retention times at 7.07, 10.07, 15.62, 16.52, and 16.63 min. Eventually, the open ring reactions proceeded, with the retention times at 6.49, 10.85, 12.91 min, most of which were inorganic acids, such as oxalic acid, and so on. Owing to the lack of responding standard chemical material, the quantification of relative intermediates was nearly impossible. The peak with $t_R = 7.20$ min might be produced by the reaction between the removal of benzene products and chlorine radical. Chlorine ion was from the dissociation of the MG, and was oxidized by hydroxyl radicals to form radical. The major ions in the mass spectra include the following (*m*/*z*, %): 146 ($(M - H)^+$; 100); 111($(M - H - Cl)^+$; 40) and 75 ($(M - 2H - 2Cl)^+$; 20). The similar product was once reported during the degradation of MG.[22] The peak with $t_R = 27.64$ min was leucomalachite green (LMG), which was the reductive transformation of MG,[15] produced by the ultraviolet irradiation. Its further demethylation was not observed at present. The major ions in the mass spectra include the following (*m*/*z*, %): 330 (M; 75); 286 ($(M - 2CH_2\text{-NH-}H)^+$; 15); 253 ($(M - C_6H_5)^+$; 100); 237(10); 209(40); 165(25).

3.6. Variations of Inorganic Ions. According to theoretical computation, once 20 ppm of MG was mineralized into dioxide carbon and water, there would be 6.81 ppm NO_3^-. During the mineralization of MG within the MPC process, the variation of inorganic ions is illustrated in the Supporting Information (Figure 7S), where NO_3^-, NO_2^-, and HCO_3^- have been assured through the comparison of retention time with external standard solution. However, there are two unidentified ions, which might be some organic acid, and it is hardly clear what the responding peaks represent. The maximum concentration C_{NO3^-} was only 4.6524 ppm. This error might be due to a radical forming under UV irradiation conditions, while some compounds with nitrite or nitrate groups were not identified. According to the literature,[29−31] nitrite or nitrate could be oxidized into nitrate radical by photogenerated holes or active radicals, which causes the decrease of NO_3^-, NO_2^- and so on. Due to further oxidation, the responding pH increased from 4.2 to 6.4, in the inset of Figure 3S in the Supporting Information.

3.7. Degradation Mechanism of MG During MPC Process. Under UV irradiation, catalysts could utilize the input energy to produce electron−hole pairs, which could transfer to the surface of catalyst. Generated holes could directly oxidize the surface-adsorbed H_2O or OH^- to produce ·OH radicals. Photoinduced electrons could be scavenged by the dissolved oxygen or other oxidants to produce superoxide anion and other reactive oxygen species (ROS), which finally could be transformed into hydroxyl radicals. Then, all kinds of ROS would induce further oxidation of MG and the intermediates, which could be adsorbed onto the surface of catalyst through the dimethylamine group. Additionally, some ROS could desorb from the surface of catalyst and oxidize all kinds of organic substances in the bulk of the solution. All the reaction routes were displayed in the Supporting Information (Scheme 1S).

On the basis of intermediates identified by LC-MS/MS and GC-MS, the reaction pathway of MG during the MPC process is described in Scheme 1, which is composed of three reaction routes. First, the cleavage of the central carbon reaction results in destruction of the conjugated structure with the main product 4-dimethylaminobenzophenone (DLBP), through the broken bond between C_1-C_4, followed by benzene removal and open ring reaction with the main products of phenol, terephthalic acid, oxalic acid, benzoic acid, terephthalic acid formate, lactic acid, etc. Second, the adduct reaction of the hydroxyl radical with MG could produce C with $m/z = 345$, H with $m/z = 361$, and

I with $m/z = 345$, which could further react with hydroxyl radicals to produce J with $m/z = 327$, K with $m/z = 313$, and L with $m/z = 299$ through dehydration reaction and *N*-demethylation reaction. The isomers of C and I mentioned above were produced due to the effect of adduct reaction of ortho position and para position and the effect of steric hindrance of the benzene ring. Third, the *N*-demethylation reaction results in a series of *N*-demethylations, which was produced through the broken bond between N(21)−C(22), N(21)−C(23), N(20)−C(24), N(20)−C(25). UV−Vis spectra of the solution displayed the blue-shift. All *N*-demethylation intermediates were degraded into small molecular species through cleavage of the central carbon reaction, benzene removal, and open ring reaction, too. Also, according to theoretical computation and bond energy analysis, MG could directly utilize ultraviolet for *N*-demethylation reaction and cleavage of the central carbon reaction in accordance with the emission spectra of EDLs, used in the MPC process.

4. Conclusions

TiO_2-based MPC degradation of MG in aqueous solutions was investigated, and the results indicated that MG was decomposed in 3 min with the corresponding TOC removal efficiency of 85%. Such satisfactory performance implied the potential of MPC degradation to treat associated dye wastewaters. Moreover, we detected four kinds of *N*-demethylation intermediates, such as DM-PM, MM-PM, M-PM, etc., and two kinds of newly detected adduct reaction products resulting from the adduct reaction of hydroxyl radical by using LC-ESI-MS techniques. Decomposition compounds of the conjugated structure (4-dimethylaminobenzophenone (DLBP)) were identified by both GC-MS and LC-ESI-MS. Other nine kinds of products from benzene removal and other open-ring intermediates such as phenol, terephthalic acid, adipic acid, benzoic acid, etc., were also detected by GC-MS. Thus, we believed that the major MG degradation routes involve five possible steps under microwave conditions: the competitive reactions between *N*-demethylation reactions, the adduct reaction and the cleavage of the central carbon, with subsequent removal of benzene and the open ring reaction, and the final mineralization process.

Acknowledgment. The authors greatly acknowledge the National Natural Science Foundation of China (20707009 and 20737001), Jiangsu Province Social Development Foundation (BS2007051), and Resource Reuse Opening Foundation (PCR-RCF07003) for financial support. We thank Professor Bing Cai Pan (Nanjing University) for his beneficial advice on the modification of this paper.

Supporting Information Available: Figure 1S describing the whole apparatus used in the MPC condition and the inset showing EDLs. Figure 2S introducing the ultraviolet light intensity of EDL-1 without solvent at 254 nm in and out of microwave oven on fixed position. Figure 3S demonstrating the emission spectra of EDL. Figure 4S showing the control experiments of microwave-assisted photocatalytic degradation of MG under different conditions. Figures 5S and 6S separately depicting the variation of main organic degradation products and inorganic ions, formed during the MPC process. Scheme 1S describing the mechanism of photocatalytic reactions. This material is available free of charge via the Internet at http://pubs.acs.org.

References and Notes

(1) Gregory, P. Dye and Dye Intermediates. In *Encyclopedia of Chemical Technology*; Kroschwitz, J. I., Ed.;Wiley: New York, 1993; Vol. 8, p 544.
(2) Srivastava, S.; Sinha, R.; Roy, D. *Toxicology* **2004**, *66*, 319.
(3) Berberidou, C.; Poulios, I.; Xekoukoulotakis, N. P. *Appl. Catal., B* **2007**, *74*, 63.
(4) Sauer, T, Cesconeto. Neto, G., José, H. J. et al. *J. Photochem. Photobiol., A: Chem.* **2002**, *149*, 147.
(5) Daneshvar, N.; Salari, D.; Khataee, A. R. *J. Photochem. Photobiol., A: Chem.* **2003**, *157*, 111.
(6) Ramakrishna, K. R.; Viraraghavan, T. *Water Sci. Technol.* **1997**, *36* (2), 189.
(7) Horikoshi, S.; Hidaka, H.; Serpone, N. *Environ. Sci. Technol.* **2002**, *36*, 1357.
(8) Horikoshi, S.; Hojo, F.; Hidaka, H. *Environ. Sci. Technol.* **2004**, *38*, 2198.
(9) Zhang, Y. B.; Quan, X.; Chen, S. *J. Hazard. Mater.* **2006**, *137*, 534.
(10) Sun, Y.; Zhang, Y. B.; Quan, X. *Sep. Purif. Technol.* **2008**, *62*, 567.
(11) Bojinova, A.; Kralchevska, R.; Poulios, I. *Mater. Chem. Phys.* **2007**, *106*, 187.
(12) Sayýlkan, F.; Asiltürk, M.; Tatar, P. *J. Hazard. Mater.* **2007**, *144*, 140.
(13) Arpaç, E.; Sayýlkan, F.; Asiltürk, M.; Tatar, P. *J. Hazard. Mater.* **2007**, *140*, 69.
(14) Sayllkan, F.; Asiltürk, M.; Tatar, P. *Mater. Res. Bull.* **2008**, *43*, 127.
(15) Ta, N.; Hong, J.; Liu, T. F. *J. Hazard. Mater.* **2006**, *B138*, 187.
(16) Gao, Z. Q.; Yang, S. G.; Ta, N. *J. Hazard. Mater.* **2007**, *145*, 424.
(17) Yang, S. G.; Fu, H. B.; Sun, C., et al. *J. Hazard. Mater.*, in press,doi: 10.1016/j.jhazmat.2008.04.107.
(18) Hong, J.; Sun, C.; Yang, S. G. *J. Hazard. Mater.* **2006**, *B133*, 162.
(19) Liu, Y. Z.; Yang, S. G.; Hong, J. *J. Hazard. Mater.* **2007**, *142*, 208.
(20) Gao, Z. Q.; Yang, S. G.; Sun, C. *Sep. Purif. Technol.* **2007**, *58*, 24.
(21) Horikoshi, S.; Kajitani, M.; Serpone, N. *J. Photochem. Photobiol., A Chem.* **2007**, *188*, 1.
(22) Chen, C. C.; Fan, H. J.; Jang, C. Y. *J. Photochem. Photobiol., A: Chem.* **2006**, *184*, 147.
(23) Chen, C. C.; Lu, C. S.; Chung, Y. C. *J. Hazard. Mater.* **2007**, *141*, 520.
(24) Pérez-Estrada, L. A.; Agüera, A.; Hernando, M. D. *Chemosphere* **2008**, *70*, 2068.
(25) Cheng, M.; Ma, W.; Zhao, J. *Environ. Sci. Technol.* **2004**, *38*, 1569.
(26) Zhang, X. W.; Wang, Y. Z.; Li, G. T. *J. Mol. Catal. A: Chem.* **2005**, *237*, 199.
(27) Horikoshi, S.; Hidaka, H.; Serpone, N. *J. Photochem. Photobiol., A: Chem.* **2002**, *153*, 185.
(28) Muller, P.; Loupy, A.; Klan, P. *J. Photochem. Photobiol., A: Chem.* **2003**, *158*, 1.
(29) Vione, D.; Maurino, V.; Minero, C. *Environ. Sci. Technol.* **2003**, *37*, 4635.
(30) Vione, D.; Maurino, V.; Minero, C.; Pelizzetti, E. *Environ. Sci. Technol.* **2002**, *36* (4), 669.
(31) Fischer, M.; Warneck, P. *J. Phys. Chem.* **1996**, *100* (48), 18749.

JP804439Z